

Enhanced skin wound healing by a sustained release of growth factors contained in platelet-rich plasma

Hee Seok Yang^{1*}, Jaehoon Shin^{1*},
Suk Ho Bhang¹, Jung-Youn Shin¹,
Jooyeon Park¹, Gun-Il Im²,
Chang-Sung Kim³ and Byung-Soo Kim^{1,4}

¹School of Chemical and Biological Engineering
Seoul National University

Seoul 151-744, Korea

²Department of Orthopaedics

Dongguk University International Hospital

Goyang 411-773, Korea

³Department of Periodontology

College of Dentistry

Yonsei University

Seoul 120-752, Korea

⁴Corresponding author: Tel, 82-2-880-1509;

Fax, 82-2-888-1604; E-mail, byungskim@snu.ac.kr

*These authors contributed equally to this work.

<http://dx.doi.org/10.3858/emmm.2011.43.11.070>

Accepted 16 August 2011

Available Online 17 August 2011

Abbreviations: BMP, bone morphogenetic protein; DAPI, 4',6-diamidino-2-phenylindole; ECM, extracellular matrix; FGF, fibroblast growth factor; HDFs, human dermal fibroblasts; HS, heparin sulfate; MMP, matrix metalloprotease; SC, subcutaneous tissue; SM, smooth muscle; vWF, von Willebrand Factor

Abstract

Platelet-rich plasma (PRP) contains growth factors that promote tissue regeneration. Previously, we showed that heparin-conjugated fibrin (HCF) exerts the sustained release of growth factors with affinity for heparin. Here, we hypothesize that treatment of skin wound with a mixture of PRP and HCF exerts sustained release of several growth factors contained in PRP and promotes skin wound healing. The release of fibroblast growth factor 2, platelet-derived growth factor-BB, and vascular endothelial growth factor contained in PRP from HCF was sustained for a longer period than those from PRP, calcium-activated PRP (C-PRP), or a mixture of fibrin and PRP (F-PRP). Treatment of full-thickness skin wounds in mice with HCF-PRP resulted in much faster wound closure as well as dermal and epidermal regeneration at day 12 compared to treatment with ei-

ther C-PRP or F-PRP. Enhanced skin regeneration observed in HCF-PRP group may have been at least partially due to enhanced angiogenesis in the wound beds. Therefore, this method could be useful for skin wound treatment.

Keywords: angiogenesis inducing agents; endothelial growth factors; fibrin; fibroblast growth factor 2; heparin; neovascularization, physiologic; platelet-derived growth factor; platelet-rich plasma; wound healing

Introduction

Clinical interest in platelet-rich plasma (PRP) stems from its potential as a safe and easily attainable source of the wide range of growth factors (GFs) and cytokines required in physiological tissue repair. PRP contains not only a number of GFs, including platelet-derived growth factor (PDGF), vascular endothelial growth factor (VEGF), transforming growth factor (TGF)- β , insulin-like growth factor (IGF), and fibroblast growth factor (FGF)-2, but also cytokines and inflammatory mediators (Rozman and Bolta, 2007). Unfortunately, the clinical evidence for PRP as a therapeutic agent is insufficient (Froum *et al.*, 2002; Raghoobar *et al.*, 2005) due to obstacles such as rapid washout (Tsay *et al.*, 2005) and inactivation (Bir *et al.*, 2009) of the critical proteins in PRP. However, there have been a few studies on the sustained delivery of GFs contained in PRP whose aims were to prevent initial washout and control the release of important proteins in PRP to the concerned area (Hokugo *et al.*, 2005).

Various heparin-conjugated biomaterials have been utilized as a GF delivery vehicle (Jeon *et al.*, 2006; Thomopoulos *et al.*, 2010; Yang *et al.*, 2010a, 2010b) by mimicking the physiological function of heparin sulfate (HS), which is abundant in the extracellular matrix (ECM). During healing, GFs are detached from and HS boosts the effect of the GFs (Schultz and Wysocki, 2009). Heparin, a well-known anticoagulant, is closely related to HS in a structural sense and can also bind to various GFs, including VEGF (Iozzo and San Antonio, 2001), PDGF (Chu *et al.*, 2004), and FGF2 (Schultz and Wysocki, 2009). Previously, we developed heparin-conjugated fibrin (HCF) and showed that

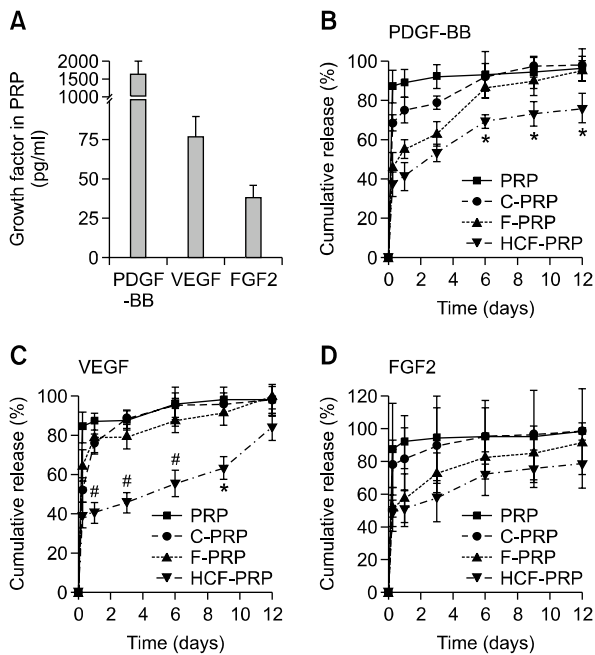


Figure 1. Release of various GFs contained in PRP from various delivery systems. (A) The concentrations of GFs in PRP. Kinetics of release of (B) PDGF-BB, (C) VEGF, and (D) FGF2 from various delivery systems *in vitro*. Values represent the mean \pm standard deviation ($n = 3$). * $P < 0.05$ compared to any group. # $P < 0.001$ compared to any group.

HCF can provide superior tissue regeneration properties to fibrin-based carriers by releasing bone morphogenic protein-2 (Yang *et al.*, 2010b) and FGF2 (Yang *et al.*, 2010a) for long time periods. In the present study, we have adopted HCF as a PRP carrier system and used it to make comparisons with other carrier systems both *in vitro* and *in vivo*. We first examined the release kinetics of GFs contained in PRP from HCF and fibrin-based carriers. Among the GFs contained in PRP, release of PDGF-BB, VEGF, and FGF2 was evaluated since these GFs can bind to heparin in HCF (Yang *et al.*, 2010a, 2010b) and are known to stimulate angiogenesis (Yang *et al.*, 2010a), which promotes skin wound healing (Tonnesen *et al.*, 2000). Activities of GFs released from the carriers were evaluated by determining the growth of human dermal fibroblasts (HDFs) cultured in the presence of GF delivery systems. To determine whether or not the delivery of GFs contained in PRP with HCF enhances wound healing as compared to calcium-activated PRP (C-PRP) or a mixture of fibrin and PRP (F-PRP), full-thickness skin wounds in mice were treated with HCF-PRP, C-PRP, or F-PRP. Calcium was added to PRP in C-PRP group to induce platelets in PRP to release growth factors (Frechette *et al.*, 2005). Fibrin was added to PRP in F-PRP group to enhance gel formation. Twelve

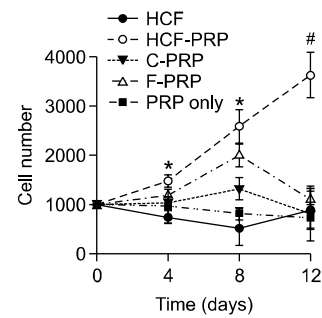


Figure 2. The bioactivity of GFs in PRP released from various delivery systems. Bioactivity of the GFs was evaluated by measuring their ability to stimulate HDF growth *in vitro*. Values represent the mean \pm standard deviation ($n = 3$). * $P < 0.05$ compared to any group. # $P < 0.01$ compared to any group.

days after treatment, skin wound healing was evaluated based on histology, morphometric analysis, immunohistochemistry, and reverse transcription polymerase chain reaction (RT-PCR).

Results

In vitro GF release

As determined by enzyme-linked immunosorbent assay (ELISA), PRP contained 1628.0 ± 381.3 ng/ml of PDGF-BB, 76.2 ± 12.9 pg/ml of VEGF, and 37.9 ± 7.8 pg/ml of FGF2 (Figure 1A). Most of PDGF-BB, VEGF, and FGF2 contained in PRP were released within 6 h when no carrier was used (Figures 1A-1D). The initial burst release and release period differed depending on the type of delivery system (Figures 1B-1D). The initial burst release for PDGF-BB and VEGF in the first 6 h from PRP, C-PRP, and F-PRP was larger than that from HCF-PRP. HCF-PRP released $69.3 \pm 3.2\%$ of PDGF-BB within 6 days, whereas approximately the same amount was released from C-PRP and F-PRP within 6 h and 3 days, respectively. HCF-PRP released $63.6 \pm 5.8\%$ of VEGF within 9 days, whereas approximately the same amount was released from C-PRP and F-PRP within 6 h.

Bioactivity of GFs released from delivery systems

The bioactivity of GFs released from the delivery systems was evaluated by determining their ability to stimulate HDF growth in the presence of each delivery system. HCF (containing no PRP) and PRP showed no cell growth (Figure 2). Cell number increased until day 8 and thereafter decreased in both C-PRP and F-PRP. In contrast, HCF-PRP resulted in sustained cell growth within the range of observation (12 days).

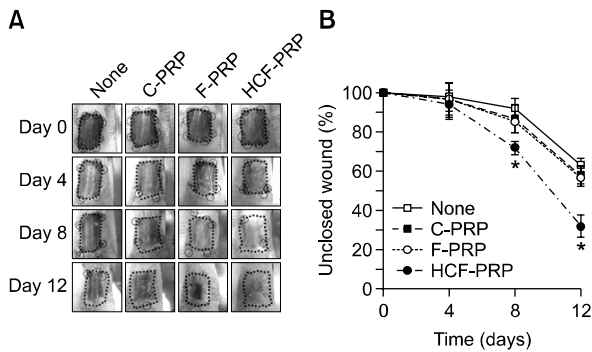


Figure 3. Wound closure. (A) Representative photographs of full-thickness skin wounds at various time points after treatment with PRP + various delivery systems. The dotted lines indicate the original wound margin. The dotted circles indicate the knots of stitches. (B) Wound closure rates. * $P < 0.05$ compared to any other group.

Macroscopic wound closure

The wound area at various times points was expressed as a percentage relative to the original wound size. Four days after treatment, the wound area was not significantly different among the groups (Figure 3). At day 8 and 12, HCF-PRP group showed significantly smaller wound size ($69.6 \pm 8.4\%$, $21.2 \pm 4.6\%$) compared to the other groups. The wound sizes of C-PRP and F-PRP groups were not significantly different from those of no treatment group at day 8 and day 12.

Histological observation

Masson's trichrome staining of histological sections of tissue taken from the center of the healed wounds at day 12 indicated that among the groups, HCF-PRP showed a histological structure most similar to that of normal skin (Figures 4A and 4B). Three different histological criteria were applied to quantitatively evaluate wound healing: hypertrophic coverage, distances between the epithelial tips, and subcutaneous tissue (SC) edges (Figure 4C). Twelve days after treatment, F-PRP and HCF-PRP showed almost complete epithelialization in the wound area, whereas no treatment and C-PRP groups still contained gaps of several millimeters between the epithelial tips (Figure 4D). Distances between the edges of SCs in HCF-PRP group were significantly smaller than those in the other three groups (Figure 4D).

Epithelial regeneration

Epithelial maturation was evaluated by immunofluorescent staining for mouse involucrin at the mid-portion of the wound at day 12 (Figure 5A). No treatment at day 0 revealed no involucrin staining.

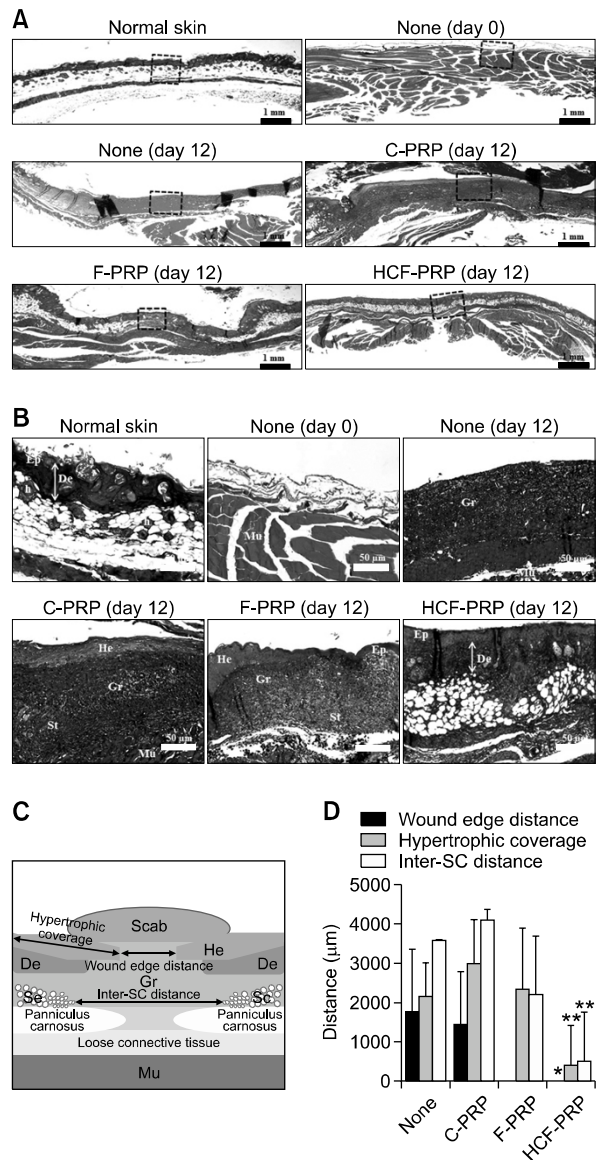


Figure 4. Histological analyses of wound healing. Masson's Trichrome-stained sections of wounds (A) at a low magnification and (B) at a high magnification at 12 days after treatment with PRP + various delivery systems. The dotted squares indicate the mid portion used in (B). Ep, epithelium; De, dermis; h, hair follicle; Gr, granulation tissue; Mu, muscle layer; Sc, subcutaneous tissue; St, scar tissue; He, hypertrophic epithelium. (C) Graphic illustration of wound healing. (D) Wound edge distance (i.e., distance between tips of epithelium), hypertrophic coverage, and inter-SC distance in wounds at 12 days after treatment with PRP + various delivery systems. * $P < 0.001$ compared to F-PRP or HCF-PRP. ** $P < 0.05$ compared to HCF-PRP.

HCF-PRP group showed an expression pattern for involucrin that was similar to that of normal skin. No treatment, C-PRP, and F-PRP groups showed only small amounts of involucrin expression. The expression level of matrix metalloprotease (MMP)-9, which is induced during keratinocyte migration (McCawley *et al.*, 1998), in the wound beds was

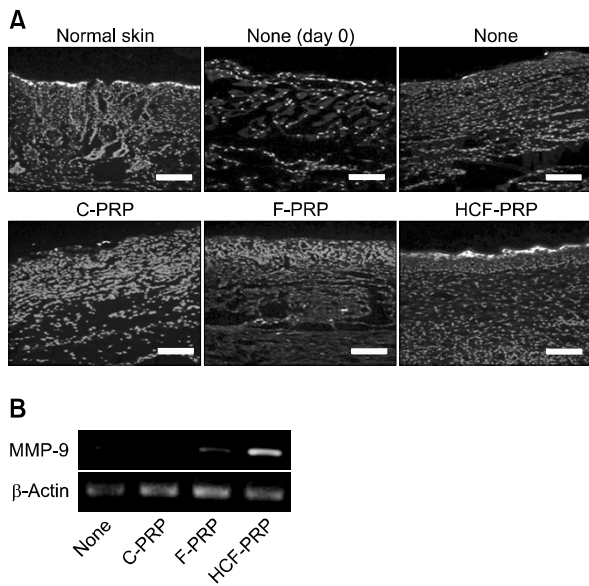


Figure 5. Epithelial regeneration in full-thickness skin wounds at 12 days after treatment with PRP + various delivery systems. (A) Immunohistochemical staining with anti-involucrin antibodies of treated wound sections. Red and blue (DAPI) indicate differentiated epithelial layer and nucleus, respectively. Scale bars indicate 100 μm . (B) RT-PCR analysis for MMP-9 expression in the wounds at 12 days after treatment with PRP + various delivery systems.

higher in HCF-PRP group compared to the other groups (Figure 5B). In no treatment and C-PRP groups, MMP-9 expression was below the detection range.

Angiogenesis

HCF-PRP enhanced angiogenesis at the wound beds as compared to no treatment, C-PRP, and F-PRP groups. Immunofluorescent staining for mouse smooth muscle (SM) α -actin and quantification of arteriole density revealed that arteriole density was significantly enhanced by HCF-PRP treatment ($3.8 \pm 1.4/\text{mm}^2$) as compared to no treatment ($0.0 \pm 0.0/\text{mm}^2$), C-PRP ($0.6 \pm 1.0/\text{mm}^2$), and F-PRP ($0.3 \pm 0.6/\text{mm}^2$) groups (Figure 6). Immunofluorescent staining for mouse von Willebrand Factor (vWF) and quantification of capillary density revealed that HCF-PRP significantly enhanced capillary density ($16.3 \pm 5.7/\text{mm}^2$) as compared to no treatment ($0.0 \pm 0.0/\text{mm}^2$), C-PRP ($0.0 \pm 0.0/\text{mm}^2$), and F-PRP ($0.4 \pm 0.7/\text{mm}^2$) groups (Figure 7).

Discussion

Although PRP is an inexpensive and immunologically safe source of GFs, the tissue regeneration efficacy of PRP has been controversial (Froum *et*

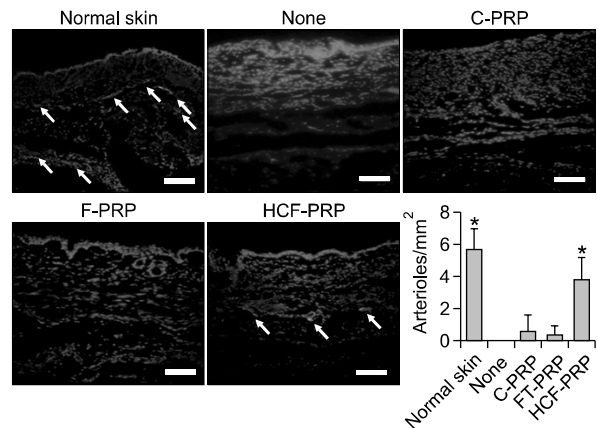


Figure 6. Neovascularization in the wounds at 12 days after treatment with PRP + various delivery systems. Immunohistochemical staining with anti-SM α -actin antibodies. Green and blue (DAPI) indicate the walls of arterioles and nucleus, respectively. Scale bars indicate 100 μm . Arteriole density was quantified. * $P < 0.05$ compared to any other group.

al., 2002; Raghoobar *et al.*, 2005) because of the rapid inactivation and initial burst of GFs contained in the PRP. During physiological wound healing, an important role of extracellular matrix (ECM) is to preserve GFs in an active state and release them when necessary (Tonnesen *et al.*, 2000). In order to preserve GF activity and secrete them to wound sites, we used HCF as a carrier for GFs contained in PRP, since HS, a natural analogue of heparin, is involved in the storage of GFs inside the ECM (Chu *et al.*, 2004; Schultz and Wysocki, 2009). The use of PRP-HCF for tissue regeneration mimics the physiological tissue regeneration process,

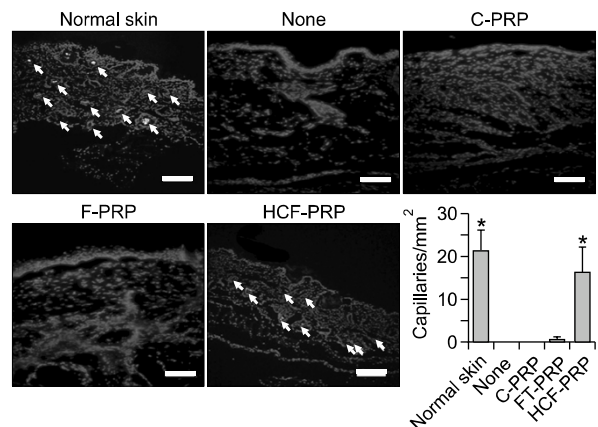


Figure 7. Neovascularization in the wounds at 12 days after treatment with PRP + various delivery systems. Immunohistochemical staining with anti-vWF antibodies. Green and blue (DAPI) indicate the walls of capillaries and nucleus, respectively. Scale bars indicate 100 μm . The capillary density was quantified. * $P < 0.05$ compared to any other group.

since PRP contains a wide spectrum of the GFs and cytokines required for tissue regeneration and HCF can mimic the role of ECM for GF release.

PRP also contains FGF2 (Bennett and Schultz, 1993; Marui *et al.*, 2005). Studies have suggested that exogenously administered FGF2 can enhance the regeneration of connective tissue in dermal wound healing models with enhanced angiogenesis (Davidson, 1988). FGF2 administered to dermal fibroblasts and keratinocytes may act in both an autocrine and paracrine fashion in promoting re-epithelialization during skin wound healing (Scott *et al.*, 1991). In our previous study, prolonged FGF2 delivery by HCF also enhanced the skin regeneration (Bhang *et al.*, 2011).

The results of the *in vitro* GF release test and bioactivity test (Figure 1) show that HCF preserved GF activity and released them slowly. The release test showed that PRP-HCF exerted sustained release of HGF, VEGF, and FGF2, which are important GFs for angiogenesis and tissue regeneration (Tonnesen *et al.*, 2000). The sustained release of GFs by HCF is attributed to electrostatic interactions between several types of GFs contained in PRP and heparin contained in HCF (Yang *et al.*, 2010a, 2010b). PRP-HCF also induced growth of HDF throughout the culture period, suggesting that HCF exerted sustained release of GFs contained in PRP and preserved the activity of the GFs. On the other hand, PRP alone did not have bioactivity on HDF growth likely due to rapid inactivation of GFs contained in PRP. Heparin contained in HCF may prevent potential loss of GF bioactivity. In the presence of heparin, degradation of bone morphogenetic protein (BMP-2) is blocked, and the half-life of BMP-2 in culture media is increased 20-fold (Zhao *et al.*, 2006).

The sustained delivery of GFs contained in PRP using HCF enhanced mouse full-thickness skin wound healing compared to delivery of GFs using either no carrier or fibrin (Figures 3-5). Based on histology, HCF-PRP group also showed shorter inter-SC distance than F-PRP and C-PRP groups (Figure 4D). This indicates that HCF-PRP promoted the recovery of normal skin structure. HCF-PRP group yielded faster epithelial closure than F-PRP and C-PRP groups (Figure 5A), indicating that HCF-PRP could accelerate keratinocyte migration to the wound site and reestablish the skin barrier, which can prevent the invasion of pathogens such as bacteria. HCF-PRP induced upregulation of the MMP-9 gene compared to no treatment, F-PRP, and C-PRP groups (Figure 5B). MMP-9 shows keratinocyte cell migration through the wound site (Tharakan *et al.*, 2010), which explains the better epithelial closure in HCF-PRP group compared to

the other groups. A study reported that FGF2 may act on keratinocytes and promote re-epithelialization during skin wound healing (Hebda *et al.*, 1990). Thus, sustained release of FGF2 by HCF may enhance re-epithelialization efficacy of PRP. Previous studies have shown that applying HCF only to skin wounds has no stimulatory effect on wound healing (Bhang *et al.*, 2011).

The enhanced wound healing may be attributed, at least in part, to enhanced neovascularization in the wound beds (Tonnesen *et al.*, 2000), which is likely due to sustained delivery of GFs contained in PRP using HCF. Neovascularization is necessary to sustain the newly formed granulation tissue in the wound region (Singer and Clark, 1999). Granulation tissue replaces the fibrin clot of the wound as phase transition occurs from inflammatory phase to proliferative phase (Baum and Arpey, 2005). Granulation tissue contains macrophages that provide GFs necessary for fibroplasia and angiogenesis, which in turn provide new ECM for cell ingrowth and supply oxygen and nutrients for cell metabolism (Singer and Clark, 1999). The enhanced neovascularization by sustained delivery of GFs contained in PRP has been also reported in a previous study demonstrating that sustained release of GFs in PRP using gelatin hydrogel enhances vessel density and perfusion in ischemic hind limbs in mice compared to treatment with PRP only (Bir *et al.*, 2009). HCF-PRP group showed enhanced neovascularization in the repair tissues as compared to no treatment, F-PRP, and C-PRP groups (Figures 6 and 7). Neovascularization process involves MMP (Raza and Cornelius, 2000). MMP-2 and MMP-9 mediate neovascularization by endothelial cell migration as they degrade ECM (Schnaper *et al.*, 1993; Raza and Cornelius, 2000; Kim *et al.*, 2010). MMPs are localized on endothelial cells by integrins such as $\alpha_v\beta_3$ (Brooks *et al.*, 1996), and MMP expression is stimulated by GFs such as VEGF and FGF (Moses, 1997). VEGF and FGF also stimulate the expression of integrins in endothelial cells (Enenstein *et al.*, 1992; Senger *et al.*, 1996, 1997). Sustained release of GFs from PRP by HCF upregulated MMP-9 expression (Figure 5B), which may promote endothelial cell migration and, in turn, neovascularization.

Although this study evaluated HCF-PRP as a wound healing material, limitations still exist. Firstly, the present study showed a superior effect of HCF-PRP on acute wound healing. However, clinical demand for newer therapeutic options is required more for chronic intractable wounds such as diabetic foot ulcer than acute injuries. PRP-HCF could be also effective for chronic wound healing, since the shortage of circulation around the chronic

wound results in a shortage of native GFs. Secondly, the present study did not clarify whether the GF-heparin complex or GF alone is released from HCF-PRP. There is a possibility that the GF-heparin complex may act as a stronger signal than GF only, similar to HS-GF complex (Schultz and Wysocki, 2009).

Methods

PRP preparation

Human blood was collected from healthy donors in an EDTA-coated container (BD Vacutainer[®], Franklin Lakes, NJ). PRP was isolated as previously described (Bir *et al.*, 2009). The blood was centrifuged at 2,400 rpm for 10 min at room temperature. After discarding the upper platelet-poor plasma, the sample was further centrifuged at 3,500 rpm for an additional 15 min, thereby separating the upper PRP layer and the lower red blood cells- and white blood cells-rich layer. The upper layer was collected carefully using an autopipette.

Preparation of HCF

HCF was prepared as previously reported (Yang *et al.*, 2010b). Heparin (molecular weight = 4,000-6,000, Sigma, St. Louis, MO) was covalently bonded to plasminogen-free fibrinogen (Sigma) using a procedure employing standard carbodiimide chemistry. HCF was formed by mixing heparin-conjugated fibrinogen (40 mg/ml), normal fibrinogen (60 mg/ml) with factor XIII, aprotinin (100 KIU/ml), calcium chloride (6 mg/ml), and thrombin (500 IU/mg) in PBS. C-PRP gel was formed by mixing 100 μ l of calcium chloride (6 mg/ml) and 100 μ l of PRP. F-PRP gel was formed by mixing 100 μ l of normal fibrinogen (60 mg/ml), thrombin (500 IU/mg), and calcium chloride (6 mg/ml) and 100 μ l of PRP. HCF-PRP gel was prepared by mixing 100 μ l of HCF and 100 μ l PRP. The volume of PRP in HCF-PRP, C-PRP, or F-PRP was half of the total volume of the gels.

Release kinetics of GFs contained in PRP

The kinetics of VEGF, FGF2, and PDGF-BB release from various delivery systems were determined by ELISA. Either 500 μ l of PRP alone or 1 ml of HCF-PRP, C-PRP, or F-PRP ($n = 3$ per group) containing 500 μ l of PRP each was gelled and immersed in 2 ml microcentrifuge tubes (Corning Inc., New York, NY) containing 1 ml of PBS. The tubes were incubated at 37°C with continuous agitation. At various time points, the supernatant was collected, and the tubes were replenished with the same amounts of fresh PBS. The amounts of VEGF, FGF-2, and HGF in the supernatants were determined using ELISA kits (R&D System, Minneapolis, MN).

Effect of GFs from PRP-loaded gels on HDF growth

The activity of GFs released from delivery systems was de-

termined by culturing HDFs in 6-well plates. PRP, C-PRP, F-PRP, or HCF-PRP ($n = 3$ per group), each containing 250 μ l of PRP, was placed in a 24 mm Transwell[®] with a 3 μ m pore polyester membrane (Corning Inc.) under which HDF was cultured. Five hundred microliters of C-PRP, F-PRP, and HCF-PRP were gelled in a discoid shape. As a negative control, 250 μ l of HCF gel without PRP was used. The medium was Dulbecco's modified Eagle's medium (DMEM, Gibco, Grand Island, NY) containing 1% penicillin/streptomycin. One thousand HDFs per well were plated and cultured. The culture medium was changed every 4 days. The cell number was counted every 3 days for 12 days using a hemocytometer (Paul Marienfeld GmbH & Co., Lauda-Königshofen, Germany).

Wound treatment

Female athymic mice (BALB/c-nu, 4 weeks old; SLC, Tokyo, Japan) were anesthetized with xylazine (20 mg/kg) and ketamine (100 mg/kg). A 2.0 \times 2.0 cm sized skin defect was made on the back of each mouse with surgical scissors. Epidermis, dermis, and SC were removed, and the muscle fascia was exposed. In order to prevent the wound by contracture, 8 sutures were placed at the border of the wound with 6-0 sutures (Ethicon, Somerville, NJ) and the wound margins were anchored to the underlying muscle fascia. The wounds were treated once with a total 200 μ l of PRP-HCF, C-PRP, and F-PRP ($n = 7$). C-PRP, F-PRP, or HCF-PRP was formed on the wounds by directly applying 100 μ l of PRP and adding 100 μ l of calcium chloride (6 mg/ml), normal fibrinogen (60 mg/ml), or HCF, respectively, on each of the wounds. The concentrations of PDGF-BB, VEGF, and FGF2 are shown in Figure 1A. After gel formation, the wounds were covered with polyurethane film (Tegaderm, 3M Healthcare, St. Paul, MN). The films covering the wounds were changed every 4 days to take macroscopic pictures of the wounds. Mice whose wounds were treated with the film only served as a negative control ($n = 7$). The animals were individually housed after surgery. The animal study procedures were approved by the Institutional Animal Care and Use Committee at Seoul National University (SNU-100629-6).

Evaluation of wound healing

At 12 days, all mice were sacrificed. The wounds were sampled in full-thickness, including the underlying muscle. Half of each specimen was used for histological analysis, and the other half was used for reverse transcriptase (RT)-PCR and immunohistochemistry. The histological specimens were fixed in formalin, embedded in paraffin, sectioned transversely at a thickness of 4 μ m, and examined with Masson's Trichrome.

Morphometric analysis

The macroscopic wound area was quantified by processing photographs taken at various time points by tracing the wound margin and calculating the pixel area relating it to the ruler using fine resolution computer mouse. The location of the advancing margin of wound closure was defined as the grossly visible margin of epithelial migration toward

the center of the wound and over the granulation tissue bed. The wound area was calculated as the percentage of the initial wound area ($[\text{wound area at time}] / [\text{initial wound area}] \times 100\%$). Microscopic tissue regeneration was determined on Masson's trichrome-stained tissue sections using a light microscope (KS400, Zeiss, Munich, Germany). Morphometric analysis was performed on digital images using the imaging software Image Pro Plus 6.0 (Mediacybernetics, Silver Spring, MD).

Immunohistochemistry

For immunohistochemical staining, samples embedded in OCT compound (Tissue-Tek 4583[®], Sakura Finetek USA Inc., Torrance, CA) were cut into 10- μm -thick sections at -22°C . To stain regenerated capillaries and arterioles, sections were immunofluorescently stained with vWF antibodies (Abcam, Cambridge, UK) and anti-SM α -actin antibodies (Abcam). The sections were also immunofluorescently stained with anti-involucrin antibodies (Abcam), which stain the stratum corneum and granulosum (Tharakan *et al.*, 2010), the more differentiated layers of the epithelium. vWF- and SM α -actin-positive signals were visualized with fluorescein-isothiocyanate-conjugated secondary antibodies (Jackson Immuno Research Laboratories, West Grove, PA). The staining signals for involucrin were visualized with rhodamine-conjugated and fluorescein-isothiocyanate-conjugated secondary antibodies (Jackson Immuno Research Laboratories). The sections were counterstained with 4',6-diamidino-2-phenylindole (DAPI) and examined by fluorescence microscopy (IX71 inverted microscope; Olympus, Tokyo, Japan). Ten slides were randomly selected from the middle part of each sample for analysis. To count capillaries and arterioles in the regenerated regions, vessels were counted and calculated as vessel number per unit area (mm^2). SM α -actin-positive vessels were counted as arterioles. The number of vWF-positive vessels minus the number of SM α -actin-positive vessels was taken as the capillary number.

RT-PCR

Total RNA was extracted from the specimen with chloroform (Sigma) and precipitated with 80% (v/v) isopropanol (Sigma). After the supernatant was removed, the RNA pellet was washed with 75% (v/v) ethanol, air-dried, and dissolved in 0.1% (v/v) diethyl pyrocarbonate-treated water (Sigma). Reverse transcription was performed using 5 μg of pure total RNA and SuperScript[™] II reverse transcriptase (Invitrogen), and the synthesized cDNA was amplified by PCR. PCR was carried out for 40 cycles of denaturation (94°C , 30 s), annealing (58°C , 45 s), and extension (72°C , 45 s) with a final extension at 72°C for 10 min. PCR products were visualized by electrophoresis on 1.5% (w/v) agarose gel followed by SYBR[®] Safe DNA gel staining (Invitrogen). The products were analyzed using a gel documentation system (Gel Doc 1000, Bio-Rad, Hercules, CA). β -actin served as an internal control. The sequences of the primers were as follows: β -actin: forward primer, 5'-TGG ACT TCG AGC AAG AGA-3'; and reverse primer, 5'-ATC TCC TTC TGC ATC CTG-3', MMP-9: forward primer, 5'-CTC AGA GAT TCT CCG TGT CCT GTA-3'; and re-

verse primer 5'-GAC TGC CAG GAA GAC ACT TGG TTA-3'.

Statistical analysis

Quantitative data were expressed as means \pm SD. Statistical comparisons were carried out using Student's *t*-test (SAS software, SAS Institute, Inc., Cary, NC). The value of $P < 0.05$ was considered statistically significant.

Acknowledgements

This work was supported by the Korea Health 21 R&D Project, Ministry of Health and Welfare (A100443).

References

- Baum CL, Arpey CJ. Normal cutaneous wound healing: clinical correlation with cellular and molecular events. *Dermatol Surg* 2005;31:674-86; discussion 686
- Bennett NT, Schultz GS. Growth factors and wound healing: Part II. Role in normal and chronic wound healing. *Am J Surg* 1993;166:74-81
- Bhang SH, Sun AY, Yang HS, Rhim T, Kim DI, Kim BS. Skin regeneration with fibroblast growth factor 2 released from heparin-conjugated fibrin. *Biotechnol Lett* 2011;33: 845-51
- Bir SC, Esaki J, Marui A, Yamahara K, Tsubota H, Ikeda T, Sakata R. Angiogenic properties of sustained release platelet-rich plasma: characterization *in vitro* and in the ischemic hind limb of the mouse. *J Vasc Surg* 2009;50:870-9 e2
- Brooks PC, Stromblad S, Sanders LC, von Schalscha TL, Aimes RT, Stetler-Stevenson WG, Quigley JP, Cheresh DA. Localization of matrix metalloproteinase MMP-2 to the surface of invasive cells by interaction with integrin alpha v beta 3. *Cell* 1996;85:683-93
- Chu CL, Buczek-Thomas JA, Nugent MA. Heparan sulphate proteoglycans modulate fibroblast growth factor-2 binding through a lipid raft-mediated mechanism. *Biochem J* 2004;379:331-41
- Davidson J, Buckley A, Woodward S, Nichols W, McGee G, Demetriou A. Mechanisms of accelerated wound repair using epidermal growth factor and basic fibroblast growth factor. *Prog Clin Biol Res* 1988;266:63-75
- Enestein J, Waleh NS, Kramer RH. Basic FGF and TGF-beta differentially modulate integrin expression of human microvascular endothelial cells. *Exp Cell Res* 1992; 203:499-503
- Frechette JP, Martineau I, Gagnon G. Platelet-rich plasmas: growth factor content and roles in wound healing. *J Dent Res* 2005;84:434-9
- Froum SJ, Wallace SS, Tarnow DP, Cho SC. Effect of platelet-rich plasma on bone growth and osseointegration in human maxillary sinus grafts: three bilateral case reports. *Int J Periodontics Restorative Dent* 2002;22:45-53
- Hebda PA, Klingbeil CK, Abraham JA, Fiddes JC. Basic

- fibroblast growth factor stimulation of epidermal wound healing in pigs. *J Invest Dermatol* 1990;95:626-31
- Hokugo A, Ozeki M, Kawakami O, Sugimoto K, Mushimoto K, Morita S, Tabata Y. Augmented bone regeneration activity of platelet-rich plasma by biodegradable gelatin hydrogel. *Tissue Eng* 2005;11:1224-33
- Iozzo RV, San Antonio JD. Heparan sulfate proteoglycans: heavy hitters in the angiogenesis arena. *J Clin Invest* 2001; 108:349-55
- Jeon O, Kang SW, Lim HW, Hyung Chung J, Kim BS. Long-term and zero-order release of basic fibroblast growth factor from heparin-conjugated poly(L-lactide-co-glycolide) nanospheres and fibrin gel. *Biomaterials* 2006;27:1598-607
- Kim S, Oh JH, Lee Y, Lee J, Cho KH, Chung JH. Induction of tissue inhibitor of matrix metalloproteinase-2 by cholesterol depletion leads to the conversion of proMMP-2 into active MMP-2 in human dermal fibroblasts. *Exp Mol Med* 2010;42:38-46
- Marui A, Kanematsu A, Yamahara K, Doi K, Kushibiki T, Yamamoto M, Itoh H, Ikeda T, Tabata Y, Komeda M. Simultaneous application of basic fibroblast growth factor and hepatocyte growth factor to enhance the blood vessels formation. *J Vasc Surg* 2005;41:82-90
- McCawley LJ, O'Brien P, Hudson LG. Epidermal growth factor (EGF)- and scatter factor/hepatocyte growth factor (SF/HGF)- mediated keratinocyte migration is coincident with induction of matrix metalloproteinase (MMP)-9. *J Cell Physiol* 1998;176:255-65
- Moses MA. The regulation of neovascularization of matrix metalloproteinases and their inhibitors. *Stem Cells* 1997;15: 180-9
- Raghoobar GM, Schortinghuis J, Liem RS, Ruben JL, van der Wal JE, Vissink A. Does platelet-rich plasma promote remodeling of autologous bone grafts used for augmentation of the maxillary sinus floor? *Clin Oral Implants Res* 2005; 16:349-56
- Raza SL, Cornelius LA. Matrix metalloproteinases: pro- and anti-angiogenic activities. *J Invest Dermatol Symp Proc* 2000;5:47-54
- Rozman P, Bolta Z. Use of platelet growth factors in treating wounds and soft-tissue injuries. *Acta Dermatovenerol Alp Panonica Adriat* 2007;16:156-65
- Schnaper HW, Grant DS, Stetler-Stevenson WG, Fridman R, D'Orazi G, Murphy AN, Bird RE, Hoythya M, Fuerst TR, French DL, *et al.* Type IV collagenase(s) and TIMPs modulate endothelial cell morphogenesis *in vitro*. *J Cell Physiol* 1993;156:235-46
- Schultz GS, Wysocki A. Interactions between extracellular matrix and growth factors in wound healing. *Wound Repair Regen* 2009;17:153-62
- Scott G, Stoler M, Sarkar S, Halaban R. Localization of basic fibroblast growth factor mRNA in melanocytic lesions by *in situ* hybridization. *J Invest Dermatol* 1991;96:318-22
- Senger DR, Ledbetter SR, Claffey KP, Papadopoulos-Sergiou A, Peruzzi CA, Detmar M. Stimulation of endothelial cell migration by vascular permeability factor/vascular endothelial growth factor through cooperative mechanisms involving the $\alpha v \beta 3$ integrin, osteopontin, and thrombin. *Am J Pathol* 1996;149:293-305
- Senger DR, Claffey KP, Benes JE, Perruzzi CA, Sergiou AP, Detmar M. Angiogenesis promoted by vascular endothelial growth factor: regulation through $\alpha 1 \beta 1$ and $\alpha 2 \beta 1$ integrins. *Proc Natl Acad Sci USA* 1997;94: 13612-7
- Singer AJ, Clark RA. Cutaneous wound healing. *N Engl J Med* 1999;341:738-46
- Tharakan S, Pontiggia L, Biedermann T, Bottcher-Haberzeth S, Schiestl C, Reichmann E, Meuli M. Transglutaminases, involucrin, and loricrin as markers of epidermal differentiation in skin substitutes derived from human sweat gland cells. *Pediatr Surg Int* 2010;26:71-7
- Thomopoulos S, Das R, Sakiyama-Elbert S, Silva MJ, Charlton N, Gelberman RH. bFGF and PDGF-BB for tendon repair: controlled release and biologic activity by tendon fibroblasts *in vitro*. *Ann Biomed Eng* 2010;38:225-34
- Tonnesen MG, Feng X, Clark RA. Angiogenesis in wound healing. *J Invest Dermatol Symp Proc* 2000;5:40-6
- Tsay RC, Vo J, Burke A, Eisig SB, Lu HH, Landesberg R. Differential growth factor retention by platelet-rich plasma composites. *J Oral Maxillofac Surg* 2005;63:521-8
- Yang HS, Bhang SH, Hwang JW, Kim DI, Kim BS. Delivery of basic fibroblast growth factor using heparin-conjugated fibrin for therapeutic angiogenesis. *Tissue Eng Part A* 2010a; 16:2113-9
- Yang HS, La WG, Bhang SH, Jeon JY, Lee JH, Kim BS. Heparin-conjugated fibrin as an injectable system for sustained delivery of bone morphogenetic protein-2. *Tissue Eng Part A* 2010b;16:1225-33
- Zhao B, Katagiri T, Toyoda H, Takada T, Yanai T, Fukuda T, Chung UI, Koike T, Takaoka K, Kamijo R. Heparin potentiates the *in vivo* ectopic bone formation induced by bone morphogenetic protein-2. *J Biol Chem* 2006;281:23246-53